Performance Assessment of Along-Track Interferometry for Detecting Ground Moving Targets

Curtis W. Chen
Jet Propulsion Laboratory, California Institute of Technology
4800 Oak Grove Drive
Pasadena, CA 91109-8099
curtis.chen@jpl.nasa.gov

Abstract— **Along-track interferometry (ATI) is an interferometric synthetic aperture radar technique that can be used to measure Earth-surface velocities. As such, the ATI technique holds promise for the detection of slowly moving ground targets. The models often used to characterize ATI performance were developed mainly in the context of mapping ocean currents, however, and they do not necessarily apply to the case of discrete, moving ground targets amidst clutter. In this paper, we provide expressions for more accurately modeling the behavior of an ATI system in the context of ground moving target indication. Analysis and design equations are given for topics including target defocus, signal-to-noise and signal-to-clutter ratios, interferometric correlation, interferometric phase bias, target detection, geolocation accuracy, and area coverage rate.**

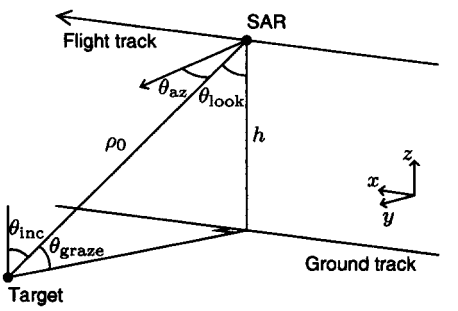

Fig. 1. Acquisition geometry used for the analysis of this paper.

I. Introduction

Along-track interferometry (ATI) is an interferometric synthetic aperture radar (InSAR, IFSAR) technique that can be used to map Earth-surface velocities. Unlike cross-track InSAR techniques that are able to map surface topography by utilizing dual-channel SAR data acquired from phase centers separated in elevation on the platform, the ATI technique involves the acquisition of data from phase centers that are separated in the direction of the platform flight path. SAR images formed from these two phase centers are therefore characterized by a temporal baseline equal to the time required for the platform to travel the distance of the along-track offset of the phase centers. Thus, while stationary elements of the imaged scene contribute identically to the two images, moving targets in the scene exhibit phase shifts between the two images. An interferogram formed from the two images consequently depicts surface movements in the imaged scene.

ATI techniques have been developed mainly in the context of mapping ocean surface currents for science applications, wherein velocity accuracies on the order of a few centimeters per second have been reported from airborne platforms [1]. There is hence great interest in using ATI techniques for ground moving target indication (GMTI), potentially from spaceborne platforms. The ATI performance models used for ocean currents do not necessarily apply to discrete ground moving targets amidst clutter, however. In this paper, we examine ATI principles in the specific context of detecting slowly moving ground targets in order to develop expressions for evaluating the expected performance of ATI techniques for such applications. The analysis presented here is meant to augment and expand upon previous studies of the subject [2]–[5]. We specifically investigate target defocusing effects, signal-to-noise and signal-to-clutter ratio (SNR, SCR) relationships, interferometric phase behavior in the presence of clutter, target detection based on interferometric data, target geolocation, and the attainable area coverage rate.

Throughout the paper, we assume that the SAR data are collected in an ideal zero-Doppler (unsquinted) stripmap mode (see [6]) as shown in Fig. 1. Most of the analysis can be adapted to other acquisitions modes or geometries as well, however. We assume that the platform follows a straight and level trajectory at a height h and velocity v_{plat}. The coordinate system is defined such that x is parallel to the platform velocity vector, y corresponds to increasing ground range, and z corresponds to height. We assume that the baseline (physical separation) between the two SAR phase centers contains only an along-track component B_x and that each phase center both transmits and receives ('ping pong' mode).

We consider only a single moving target, at a broadside slant range ρ_0 from the platform. The target is viewed from a look angle (off-nadir angle) θ_{look}, with $\cos\theta_{\text{look}} = h/\rho_0$. For our flat-Earth geometry, the look angle is equal to the ground incidence angle θ_{inc} and complementary to the grazing

angle θ_{graze}. The off-broadside angle within the slant plane is denoted θ_{az}. The Cartesian velocity components of the target are given by v_x, v_y, and v_z, implying that the target radial velocity (*i.e.*, the slant-range projection of the target velocity) is given by

$$v_\rho = -v_z \cos\theta_{\text{inc}} + v_y \sin\theta_{\text{inc}}. \tag{1}$$

The target velocity is assumed to be constant. In the ideal case, the interferometric phase ϕ_v due to the target velocity is given by

$$\phi_v = \frac{4\pi}{\lambda}\frac{B_x}{v_{\text{plat}}}v_\rho \tag{2}$$

with a possible sign flip depending on the convention used for interferogram formation. The ambiguous ATI velocity is that which results in 2π rad of interferometric phase:

$$v_{\text{ambig}} = \frac{\lambda v_{\text{plat}}}{2B_x}. \tag{3}$$

The system can therefore observe velocities unambiguously if $-v_{\text{ambig}}/2 < v_\rho < v_{\text{ambig}}/2$.

II. Performance Relationships

We now describe a number of performance-limiting effects and provide expressions characterizing these phenomena and their impact on ATI GMTI.

A. Defocus

Before an interferogram can be formed, focused SAR imagery must be obtained. There are various mechanisms by which moving targets will be improperly focused, however.

1) Along-track velocity: A moving target will be smeared in the along-track direction if its along-track velocity component v_x is large enough that the phase history of the moving target does not match the reference phase-history function ϕ_{ref} used for SAR azimuth compression. Using a quadratic approximation, ϕ_{ref} is given by

$$\phi_{\text{ref}} = -\frac{4\pi}{\lambda}\frac{x^2}{2\rho_0} = -\frac{4\pi}{\lambda}\frac{v_{\text{plat}}^2 t^2}{2\rho_0} \tag{4}$$

where t denotes time. Neglecting across-track target velocity components, the target phase history is given by

$$\phi_{\text{tgt}} = -\frac{4\pi}{\lambda}\frac{(v_{\text{plat}} - v_x)^2 t^2}{2\rho_0}. \tag{5}$$

The phase error ϕ_{err} at the ends of the synthetic aperture is thus

$$\phi_{\text{err}} = -\frac{2\pi}{\lambda\rho_0}\left[v_{\text{plat}}^2 - (v_{\text{plat}} - v_x)^2\right]\left(\frac{T_{\text{int}}}{2}\right)^2 \tag{6}$$

where T_{int} is the SAR integration time, related to the along-track antenna length L (for stripmap systems) by

$$T_{\text{int}} = \frac{\lambda\rho_0}{L v_{\text{plat}}}. \tag{7}$$

Requiring ϕ_{err} to be less than $\pi/2$ rad and assuming that $v_{\text{plat}} \gg v_x$, Eq. (6) can be solved for v_x to give the condition that

$$|v_x| \le \frac{L^2 v_{\text{plat}}}{2\lambda\rho_0}. \tag{8}$$

This condition is equivalent to the rule of thumb that the fractional Doppler rate error, which is proportional to v_x/v_{plat}, should be less than approximately one part in the azimuth time-bandwidth product.

2) Radial velocity: A target will also appear smeared in the along-track direction due to its velocity v_ρ in the slant-range direction. This target velocity component gives rise to an additional linear term on the target phase history, thereby changing the Doppler centroid of the target. The Doppler spectrum of the target will consequently be shifted with respect to the Doppler spectrum of the clutter. Let Q_{Dop} be the fractional shift of the target Doppler spectrum, given by the ratio of the target Doppler due to radial motion to the Doppler bandwidth:

$$Q_{\text{Dop}} = \left|\frac{2v_\rho/\lambda}{2v_{\text{plat}}/L}\right| = \left|\frac{v_\rho L}{v_{\text{plat}}\lambda}\right|. \tag{9}$$

Because the SAR images will generally be processed to the Doppler centroid of the clutter, only a fraction $1 - Q_{\text{Dop}}$ of the target spectrum will be correctly processed, so the along-track resolution of the target will become coarser by a factor of $1/(1 - Q_{\text{Dop}})$. Moreover, the single-pixel SNR of the target will decrease by a factor of $(1 - Q_{\text{Dop}})^2$. That is, if $Q_{\text{Dop}} = 0.5$, the target would be smeared into two along-track resolution elements, and the total signal energy in the image would decrease by -3 dB, so the signal energy in each target pixel would decrease by a net -6 dB. An approach to avoid this effect would be to increase the bandwidth of the azimuth matched filter, but doing so would also result in an increase in the noise level proportional to the fractional increase in the filter bandwidth.

Here, we assume that the target moves slowly enough that Q_{Dop} is small. Targets that are fast enough to violate this condition would probably be detected easily with exoclutter MTI techniques in any case.

3) Range migration: It has been suggested [4] that the additional range migration due to the radial velocity v_ρ of a moving target will cause the target to be defocused in the range dimension as well. This is not the case as long as $Q_{\text{Dop}} < 1$, however, as even stationary clutter cells experience range migration over the synthetic aperture, and range migration correction is normally an integral part of SAR processing. The key point here is that the range migration due to the target radial velocity exactly matches that of some clutter cell elsewhere in the scene—otherwise, azimuth compression based on the target phase history would be impossible, as phase is a function of range. Thus, moving targets will appear well focused in range as long as their Doppler spectra do not wrap modulo the PRF.

If the targets do wrap modulo the PRF, then the *uncompensated* range migration $\Delta\rho_n$ between pulses is given by

$$\Delta\rho_n = n_{\mathrm{Dop}}\frac{\lambda}{2} \tag{10}$$

where n_{Dop} is the integer number of PRF multiples by which the target Doppler is offset from the processed Doppler. The total apparent range extent ρ_n traversed by the target over the synthetic aperture time is thus

$$\rho_n = \Delta\rho_n T_{\mathrm{int}}\mathrm{PRF} = n_{\mathrm{Dop}}\frac{\lambda^2\rho_0\mathrm{PRF}}{2Lv_{\mathrm{plat}}}. \tag{11}$$

B. SNR and SCR

The SNR and the SCR, and implicitly the clutter-to-noise ratio (CNR), are important parameters determining the interferometric performance of an ATI GMTI system, so a few comments about these quantities are warranted. We define the signal as the portion of the radar return from the moving target of interest within a particular pixel. As the radar cross section σ_{tgt} of a target generally fluctuates, the signal power is a statistical quantity whose mean is S. The clutter (which is in fact the signal in other SAR applications) is defined as the portion of the radar return from the nominally stationary ground surface, with a mean power C. We assume that the system noise in each SAR channel is independent white Gaussian noise with mean power N. The SNR, SCR, and CNR are hence defined as S/N, S/C, and C/N.

For targets that are smaller than the image resolution and not defocused by the phenomena above, the SCR is given by

$$\mathrm{SCR} = \frac{\sigma_{\mathrm{tgt}}}{\sigma_0\delta_x\delta_\rho/\sin\theta_{\mathrm{inc}}} \tag{12}$$

where σ_0 is the normalized cross section of the clutter and δ_x and δ_ρ are the along-track and slant-range image resolutions, assuming that the clutter is well focused.

Note that the effective size of a target may be different than the physical size of the target since only a portion of the target may dominate the target's microwave scattering at a given wavelength. The size of the target in relation to the resolution is also an important consideration if multiple spatial looks are desired. If the target only occupies a single resolution cell, spatial looks may not offer much benefit.

It has been suggested [2] that if the physical size of the target is approximately equal to the size of a resolution cell, the target would obscure most of the clutter patch, giving a higher SCR. This is not the case, however, as the clutter that competes with a moving target in a particular SAR image pixel is not at the same physical location as the target. That is, moving targets appear shifted in the along-track direction in SAR imagery (see below), so the clutter obscured by the target corresponds to a different image cell than the one containing the target.

On the other hand, if the target is obscured by clutter (as in the case of a target under foliage), the SCR decreases in proportion to the decrease in radar energy incident upon the target.

C. Interferometric Phase

Perhaps the most significant way in which the use of ATI techniques for moving target detection differs from its use for ocean-current applications is the presence of clutter. Because stationary clutter should be well correlated between the two images comprising the interferogram, clutter cannot be treated in the same manner as thermal noise in describing the statistics of the interferometric phase.

Consider an image cell that contains a moving target. The complex image values a_1 and a_2 of the two images will be

$$a_1 = s_1 + c + n_1 \tag{13}$$

and

$$a_2 = s_2 + c + n_2 \tag{14}$$

where s_1 and s_2 are the target signal components of the observed data, with

$$s_2 = s_1\exp(-j\phi_v); \tag{15}$$

c is the clutter contribution which, in the ideal case, is identical between the two channels and uncorrelated with the signal; n_1 and n_2 are noise terms which are independent of the signal, the clutter, and each other. The complex correlation coefficient γ_{tgt} for the cell is given by

$$\gamma_{\mathrm{tgt}} = \frac{\langle a_1 a_2^*\rangle}{\sqrt{\langle a_1 a_1^*\rangle\langle a_2 a_2^*\rangle}} \tag{16}$$

where $\langle\cdot\rangle$ denotes expectation and * denotes complex conjugation. Substituting Eqs. (13) and (14) into Eq. (16), expanding, switching the order of expectation and addition, and neglecting the covariances of uncorrelated terms, we obtain the following expression for the complex correlation coefficient

$$\gamma_{\mathrm{tgt}} = \frac{\langle s_1 s_2^*\rangle + \langle cc^*\rangle}{\sqrt{\left(\langle s_1 s_1^*\rangle + \langle cc^*\rangle + \langle n_1 n_1^*\rangle\right)\left(\langle s_2 s_2^*\rangle + \langle cc^*\rangle + \langle n_2 n_2^*\rangle\right)}} \tag{17}$$

which simplifies to

$$\gamma_{\mathrm{tgt}} = \frac{S\exp(j\phi_v) + C}{S + C + N} \tag{18}$$

where

$$N = \langle n_1 n_1^*\rangle = \langle n_2 n_2^*\rangle, \tag{19}$$

$$C = \langle cc^*\rangle, \tag{20}$$

$$S = \langle s_1 s_1^*\rangle = \langle s_2 s_2^*\rangle, \tag{21}$$

and

$$S\exp(j\phi_v) = \langle s_1 s_2^*\rangle. \tag{22}$$

The complex correlation coefficient can also be rewritten

$$\gamma_{\mathrm{tgt}} = \frac{\mathrm{SCR}\exp(j\phi_v) + 1}{\mathrm{SCR} + 1 + 1/\mathrm{CNR}}. \tag{23}$$

Equation 18 accounts for the correlated nature of the clutter and differs from the expression used in previous studies [4], [5]. As the clutter contribution goes to zero, the expression reduces to the familiar expression for interferometric coherence.

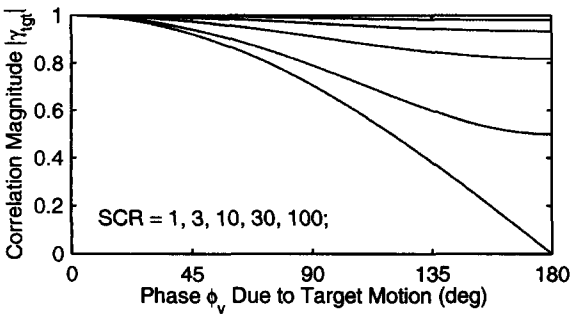

Fig. 2. Magnitude of the interferometric correlation coefficient $|\gamma_{\text{tgt}}|$ as a function of ϕ_v from Eq. (18) for various SCR values (lower curves correspond to lower SCR values). The SNR is assumed to be infinite.

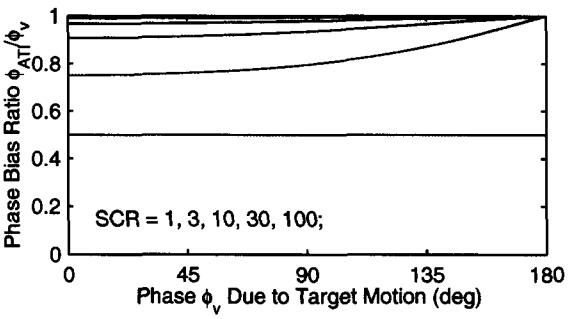

Fig. 3. Interferometric phase bias ratio ϕ_{ATI}/ϕ_v as a function of ϕ_v from Eq. (24) for various SCR values (lower curves correspond to lower SCR values).

Note that if noise is negligible, the magnitude of the correlation coefficient becomes unity both as the SCR goes to zero and as the SCR goes to infinity; this is because in either case, only one term dominates the interferometric phase. When the SCR is on the order of unity, however, the target and the clutter signatures compete against one another, and the interferogram coherence can degrade significantly. Curves of the correlation magnitude $|\gamma_{\text{tgt}}|$ are shown as a function of ϕ_v for various values of the SCR and assuming infinite SNR in Fig. 2.

The phase of the complex correlation coefficient is the expected phase of the interferogram, and Eq. (18) suggests that the expected interferometric phase ϕ_{ATI} will be a biased estimate of the phase ϕ_v due to the target velocity:

$$\phi_{\text{ATI}} = \arg(\gamma_{\text{tgt}}) = \tan^{-1}\left(\frac{S\sin\phi_v}{S\cos\phi_v + C}\right). \tag{24}$$

(A four-quadrant arctangent operation is assumed.) The bias is evident by the fact that the expected phase ϕ_{ATI} is not equal to the true moving-target phase ϕ_v. For small values of ϕ_v corresponding to slow target velocities, a small-angle approximation gives

$$\phi_{\text{ATI}} \approx \frac{S}{S+C}\phi_v \tag{25}$$

or

$$\phi_{\text{ATI}} \approx \frac{\text{SCR}}{\text{SCR}+1}\phi_v. \tag{26}$$

The interpretation of Eq. (24) is that in presence of a moving target, the expected phase of the observed data may be significantly biased towards zero—which corresponds to a lack of target motion—if the SCR is marginal. Moving targets therefore become more difficult to detect than would be expected from a model which accounts only for the phase variance (as a function of the magnitude of the correlation coefficient, $|\gamma_{\text{tgt}}|$) and not for the phase bias. Curves of the ratio ϕ_{ATI}/ϕ_v are shown as a function of ϕ_v in Fig. 3 for various values of the SCR. The bias becomes less significant as the SCR increases.

Note that the expressions derived here for the interferometric coherence and the phase bias do not assume any particular forms for the statistical distributions of the target and the clutter.

It is important to note that while multilook processing might in some cases reduce the variance of the interferometric phase, it does not mitigate bias effects. Therefore, the performance of techniques based on subbanding the SAR data must be carefully considered. That is, from Eq. (12), each of the subband interferograms will have a lower SCR because of its coarser resolution and will consequently exhibit a more significant phase bias. Multilook processing on the subband images may subsequently reduce the phase variance, but the multilook result will converge upon the more biased phase value corresponding to the lower SCR. Multilook processing does also affect the phase behavior of clutter-only cells, however, as described below.

A related observation is that estimating the true statistical correlation γ_{tgt} from observed data would be difficult because of the lack of signal stationarity. That is, insufficient data exist for an accurate estimation of γ_{tgt} because the target is contained in only a small number of resolution cells.

D. Target Detection

The statistical description of the problem of detecting moving targets based on interferometric data depends upon the assumptions made for the clutter and target statistics. Gaussian models for the ground surface are often used in SAR applications, and analytical expressions exist for the single-look and multilook phase probability density functions (PDFs) [7], [8]. If a Gaussian model is adopted for the clutter, these PDFs would apply to the clutter-only case (when no target is present), in which the interferogram coherence would be given by the usual expression

$$\gamma_{\text{clut}} = \frac{1}{1+1/\text{CNR}}. \tag{27}$$

In our ideal case, γ_{clut} is always purely real, so the clutter-only phase PDF peaks at zero.

In the target-present case, the statistics of the observed phase naturally depend on the statistics of the target. If the target is assumed to follow Gaussian statistics (corresponding to an exponential intensity distribution and a Rayleigh amplitude

distribution), the phase PDF is again given by the expressions cited above, but with different parameters for the distribution. Namely, the correlation magnitude is given by $|\gamma_{\text{tgt}}|$, as computed from Eq. (18), and the location of the PDF peak is given by Eq. (24).

The clutter-only and target-present PDFs can then be used to compute the probability of false alarm P_{FA} and the probability of detection P_D given values for the target velocity, SNR, SCR, number of looks, and a decision threshold ϕ_D on the phase. That is, if the absolute value of the observed phase is greater than ϕ_D, a target is assumed to be present.

While some of the expressions for the phase PDFs given in [7] are somewhat complicated, it is important to note that a normal approximation for the single-look clutter-only case should be avoided. This is because the tails of the single-look phase distribution do not fall off very quickly, so values computed for P_{FA} may be incorrect if a normal approximation is adopted.

The tails of the single-look clutter-only phase PDF in fact suggest that very low false alarm rates (less than about 10^{-1}) may be unreasonable even for very high CNRs [5]. The qualitative explanation for this behavior is that, even with a high CNR, many pixels in a single-look SAR image appear dark because of speckle, and the phase values of these dark pixels are well distributed over the entire $[0, 2\pi)$ interval. This is evident upon inspection of the joint PDF of the interferogram magnitude and interferogram phase [8].

This relationship between the magnitude and phase statistics suggests that the optimal decision strategy for target detection should include an examination of the interferogram magnitude as well as the interferogram phase. (We assume that the interferogram magnitude is approximately equal to the intensities of the individual SAR images.) In other words, instead of a single decision threshold ϕ_D on the interferogram phase, the decision might be based on whether the phase exceeds some threshold *and* the interferogram magnitude exceeds a magnitude threshold M_D. Such an approach would offer better detection performance than a phase-only approach.

More generally, if detection decisions are to be based on both the interferogram magnitude and phase, more complicated decision schemes than one with fixed thresholds ϕ_D and M_D can be envisioned. Such strategies would offer even better performance, although determining an optimal decision strategy based on the two variables (magnitude and phase) is not a straightforward task. Whereas in the phase-only case, a specification on either P_D or P_{FA} establishes the value of ϕ_D, there are different contours in the complex plane that can be used as decision thresholds to give the same values of P_D or P_{FA} in the two-variable decision problem.

Because the presence of a moving target reduces the interferometric correlation as described above, detection based on the estimated coherence is also possible in principle. The difficulty of accurately estimating γ_{tgt} (see above) may preclude this approach, however.

One final note on target detection requirements is in order. In an operational GMTI system, the false alarm rate may need to be linked to the SAR image resolution. This is because each pixel in the interferogram corresponds to a decision. Thus, even with a false alarm rate as low as 10^{-6}, the probability of a false alarm over a modestly sized interferogram, which could easily contain 10^6 pixels, would still be very high. Perhaps a more appropriate quantification of the desired false alarm performance would be a specification on the number of false alarms per unit area on the ground.

E. Geolocation

The detection of a moving target does not necessarily imply that its velocity can be measured if clutter is present, so an ATI system might not necessarily be able to accurately geolocate moving targets. As stated above, a moving target will appear in a SAR image at an apparent position that is shifted in the along-track direction from the true target location. This along-track shift is such that the Doppler frequency due to the target radial motion matches the Doppler frequency of a ground point elsewhere in the beam at an angle θ_{az}:

$$\frac{-2v_\rho}{\lambda} = \frac{2v_{\text{plat}} \sin\theta_{\text{az}}}{\lambda}. \tag{28}$$

The apparent target offset x_{offset} is thus given by

$$x_{\text{offset}} = \rho_0 \sin\theta_{\text{az}} = -\rho_0 \frac{v_\rho}{v_{\text{plat}}}, \tag{29}$$

assuming that the target Doppler spectrum does not wrap. Note that x_{offset} is bounded because the bandwidth of the SAR azimuth-compression filter limits the range of velocities for which targets are visible.

If the target velocity is known, as from the interferogram phase in the case of high SCR (and high SNR), the offset can be computed from Eq. (29), and the true target location can be determined [3]. If the SCR is not very high, however, the observed phase is a function of contributions from both the target and the clutter. Because the intensities of both the target and the clutter fluctuate, the relative contributions of each cannot be distinguished, and the geolocation accuracy is limited by the accuracy with which the target velocity can be determined. Note that only one or perhaps a few pixels contain target energy, so the sample support for a statistical estimation of the target velocity will likely be insufficient.

F. Area Coverage Rate

We define the area coverage rate (ACR) as the ground area that can be scanned per unit time. For a fixed-size area of interest A_{AOI}, the update rate for target tracking is therefore approximately $\text{ACR}/A_{\text{AOI}}$. Note that target tracking would require squinted operation, which we have not considered here.

The ACR of a SAR system is related to the achievable azimuth resolution because of range-Doppler ambiguities. As the azimuth resolution is linked to the SCR, we now derive a bound on the attainable ACR for an ATI GMTI system. For a stripmap SAR system, the along-track resolution δ_x is given (approximately) by

$$\delta_x = \frac{L}{2} \tag{30}$$

where, as above, L is the along-track length of the radar antenna aperture. The slant-range resolution is given by

$$\delta_\rho = \frac{c_0}{2B} \tag{31}$$

where c_0 is the speed of light and B is the pulse bandwidth. Substituting these two expressions into Eq. (12) gives

$$\mathrm{SCR} = \frac{4B\sigma_{\mathrm{tgt}} \sin\theta_{\mathrm{inc}}}{c_0\sigma_0 L}, \tag{32}$$

which can be rearranged to obtain an expression for the desired antenna length in terms of the SCR, the pulse bandwidth, and the target and clutter cross sections:

$$L = \frac{4B\sigma_{\mathrm{tgt}} \sin\theta_{\mathrm{inc}}}{c_0\sigma_0 \mathrm{SCR}}. \tag{33}$$

Let w be the antenna width in the elevation direction. The ground-range width W_y of the stripmap SAR swath is related to the antenna width by

$$W_y = \frac{\lambda\rho_0}{w\cos\theta_{\mathrm{inc}}}, \tag{34}$$

so

$$w = \frac{\lambda\rho_0}{W_y\cos\theta_{\mathrm{inc}}}. \tag{35}$$

Now, consider the minimum antenna area A_{ant} required to avoid range-Doppler ambiguities (see [6], p. 274):

$$A_{\mathrm{ant}} = wL \geq \frac{4v_{\mathrm{plat}}\lambda\rho_0 \tan\theta_{\mathrm{inc}}}{c_0}. \tag{36}$$

Substituting Eqs. (33) and (35) into Eq. (36) gives

$$\frac{\lambda\rho_0}{W_y\cos\theta_{\mathrm{inc}}}\frac{4B\sigma_{\mathrm{tgt}}\sin\theta_{\mathrm{inc}}}{c_0\sigma_0\mathrm{SCR}} \geq \frac{4v_{\mathrm{plat}}\lambda\rho_0\tan\theta_{\mathrm{inc}}}{c_0}. \tag{37}$$

The ACR for a stripmap SAR is given by

$$\mathrm{ACR} = W_y v_{\mathrm{plat}}, \tag{38}$$

so substituting Eq. (38) into Eq. (37) and solving for the area coverage rate gives

$$\mathrm{ACR} \leq \frac{\sigma_{\mathrm{tgt}}B}{\sigma_0\mathrm{SCR}}. \tag{39}$$

This expression represents an upper bound on the instantaneous ACR placed on an ATI GMTI system by the desired SCR. The bound can be understood qualitatively by observing that ATI techniques depend upon long coherent integration times in order to reduce clutter contributions to the Doppler cell of the target; the long integration times drive the ACR.

Note that Eq. (39) assumes that the radar is operated unambiguously and that the target is contained completely within a single resolution cell so that Eq. (12) applies. The expression also neglects oversampling factors, beam-broadening factors, *etc.* that would decrease the area coverage rate slightly.

While derived for a stripmap system, Eq. (39) can be alternatively derived for a spotlight SAR system by noting that

$$\delta_x = \frac{\lambda\rho_0}{2v_{\mathrm{plat}}T_{\mathrm{int}}} \tag{40}$$

and

$$\mathrm{ACR} = \frac{W_x W_y}{T_{\mathrm{int}}}. \tag{41}$$

The area coverage rate might be improved with the use of vernier or digital beamforming techniques [9], but the effects of such techniques on the interferometric phase of moving targets requires investigation.

III. Conclusions

ATI techniques hold promise for detecting slowly moving ground targets, but the traditional models for ATI performance used in the context of ocean-current measurement are not always applicable to GMTI scenarios. In order to evaluate the performance of an ATI GMTI system, the discrete nature of targets and the dominating presence of clutter in the data must be incorporated into performance models.

In this paper, we have examined several phenomena which collectively influence the performance of an ATI GMTI system. Expressions were given for relating system parameters to target defocus, SNR and SCR, interferometric correlation, interferometric phase bias, target detection, geolocation accuracy, and area coverage rate. We hope that these expressions will provide a more complete means of characterizing ATI GMTI system behavior.

As the analyses presented here are based on the geometry and models described in Section I, however, the results may be in need of refinement if the underlying assumptions regarding the system do not hold. This is the subject of continuing work.

Acknowledgment

This work was performed at the Jet Propulsion Laboratory, California Institute of Technology, under a contract with the National Aeronautics and Space Administration.

References

[1] R. M. Goldstein and H. A. Zebker, "Interferometric Radar Measurements of Ocean Surface Currents", *Nature*, **328**, 707–709, 1987.

[2] C. E. Livingstone, I. Sikaneta, C. H. Gierull, S. Chiu, A. Beaudoin, J. Campbell, *et al.*, "An Airborne Synthetic Aperture Radar (SAR) Experiment to Support RADARSAT-2 Ground Moving Target Indication (GMTI)," *Canadian Journal of Remote Sensing*, **28**, 794–813, 2002.

[3] H. Breit, M. Eineder, J. Holzner, H. Runge, and R. Bamler, "Traffic Monitoring Using SRTM Along-Track Interferometry," International Geoscience and Remote Sensing Symposium, IGARSS, Toulouse, France, July, 2003.

[4] A. A. Thompson and C. E. Livingstone, "Moving Target Performance for RADARSAT-2," International Geoscience and Remote Sensing Symposium, IGARSS, Honolulu, Hawaii, July, 2000.

[5] V. Pascazio, G. Schirinzi, and A. Farini, "Moving Target Detection by Along Track Interferometry," International Geoscience and Remote Sensing Symposium, IGARSS, Sydney, Australia, July, 2000.

[6] J. C. Curlander and R. N. McDonough, *Synthetic Aperture Radar: Systems and Signal Processing*, Wiley, New York, 1991.

[7] J. S. Lee, K. W. Hoppel, S. A. Mango, and A. R. Miller, "Intensity and Phase Statistics of Multilook Polarimetric and Interferometric SAR Imagery," *IEEE Transactions on Geoscience and Remote Sensing***32**, 1017–1028, 1994.

[8] R. Touzi and A. Lopes, "Statistics of the Stokes Parameters and of the Complex Coherence Parameters in One-Look and Multilook Speckle Fields," *IEEE Transactions on Geoscience and Remote Sensing*, **34**, 519–531, 1996.

[9] M. Younis, C. Fischer, and W. Wiesbeck, "Digital Beamforming in SAR Systems," *IEEE Transactions on Geoscience and Remote Sensing*, **41**, 1735–1739, 2003.

Subject: Document for Review
From: "Curtis W. Chen" <Curtis.W.Chen@jpl.nasa.gov>
Date: Thu, 22 Jan 2004 17:18:00 -0800
To: docrev@jpl.nasa.gov

Hello

The attached paper is to be published in the conference proceedings of the 2004 IEEE Radar conference (please note that I submitted a different paper for the same conference for review on 1/20/04). The abstract for this paper/presentation was cleared on 9/24/03 as CL#03-2595. An updated Form 1330 and the IEEE copyright form are attached.

-Curtis Chen

x4-8034
MS 300-235